Proceedings of IOE Graduate Conference, 2019-Summer
Peer Reviewed
Year: 2019 Month: May Volume: 6
ISSN: 2350-8914 (Online), 2350-8906 (Print)

Slant Crack Detection in Shaft Using Analytical Vibration Methods

Manoj Adhikari [a], Prajwal Raj Shakya [b]

[a, b] *Department of Automobile and Mechanical Engineering, Thapathali Campus, IOE, Tribhuvan University, Nepal*
Corresponding Email: [a] manojadhikari123i8@gmail.com

Abstract
Shaft is use to transmit torque and power between two components of the drive train. Due to the cyclic torsional moment, slant crack in such shaft is inevitable. In this research, a new analytical approach is developed for the detection of slant crack present in the shaft based on the dynamic response of the cracked shaft. Presence of crack in the shaft introduces local flexibility due to the strain energy concentration in the vicinity of crack tip under load. The magnitude of additional flexibility due to the crack is found from linear elastic fracture mechanics. Flexibility matrix for the cracked shaft is found to be more populated than that of the healthy shaft. The obtained flexibility matrix is incorporated into the equation of motion of the shaft and equation of motion is solved to get the dynamic response of the cracked rotor. It was found that the natural frequency and amplitude of vibration of the cracked shaft is reduced as compared to those of a healthy shaft and such response can be used for crack detection in the shaft.

Keywords
Slant Crack, Dynamic Response, Linear Elastic Fracture Mechanics, Flexibility Matrix

1. Introduction

Shaft is used to connect two components of the drive train located at certain distance and since it is a primary component used in high – performance rotating equipments such as turbines, generators, pumps and compressors etc. It is used to transmit torque and power so, it is subjected to torsion and shear stress. Fatigue cracks in such shafts are inevitable because of manufacturing defects, cyclic stress and presence of stress raisers [1]. Crack oriented at an angle of 45^0 to the axis of shaft occur from the fatigue of shaft due to the torsional moment [2]. If the crack remains undetected, it can lead to catastrophic failure causing huge loss of man, material and money so, the early detection of crack becomes necessary to prevent such disasters. Several researchers have therefore conducted extensive investigation on the response of cracked rotor over the last four decades. An in-depth literature review on dynamic of cracked shaft was published by [3] and he concluded that the basic method for dealing with the problems related to the crack detection are equivalent reduced cross section, local flexibility from fracture mechanics and cracked continuous beam or bar. Similarly, review on cracked shaft detection and diagnostics was published by [1], grouping the literatures under vibration based methods, modal testing and non-traditional methods. Research done by [4] shows that widely used way for the determination of flexibility of cracked shaft is linear elastic fracture mechanics because, it is simple and highly accurate, it doesn't change the mass of structure, can revel any non-linearity of vibration and accurate predict the change in natural frequencies and mode shape in case of fatigue cracks.

Investigation of transverse crack signature using transverse and torsional experiment was carried out by [5]. From his experimentation, it was found that due to the presence of crack the decrease in natural frequency and peak amplitude occur and for the same crack depth, the crack at middle position had the greatest reduction in natural frequency and acceleration. Similarly, the variation of location and depth of transverse crack on natural frequency was studied by [6], and it was found that, with increase in depth of the crack natural frequency value decreases and the crack in middle of the shaft pose greatest threat to the shaft.Dynamic response of the Jeffcott rotor was studied by [7],in his study, he had compared

the effect of slant crack and transverse crack on the dynamic response of Jeffcott rotor. It was found that the flexibility matrix for slant crack is more populated than that of the transverse crack. Various researchers[8] [9] [10] concluded that the existence of a crack in the shaft introduces coupling between different kind of vibration; this can form the basis of crack identification in the rotating shaft.

This paper deals with the detection of slant crack oriented at 45^0 to the axis of shaft utilizing the vibration methods because vibration method of crack detection facilitates the in operation detection of crack present in the shaft [8]. The flexibility matrix of such shaft is derived based on linear elastic fracture mechanics. The equation of motion of Jeffcott rotor is derived by considering three degree of freedom and response in time domain is plotted for both the healthy as well as for the cracked shaft where the effect of unbalance and gravity are also considered.

2. Flexibility of Cracked Rotor Shaft

Simple Jeffcott rotor model with flexible shaft is used for the analysis is shown in the figure 1 below. In this research work a shaft having a slant crack at its middle and oriented at an angle of 45^0 with the shaft axis is considered. The amount of change in flexibility due to the presence of crack is formulated using linear elastic fracture mechanics.

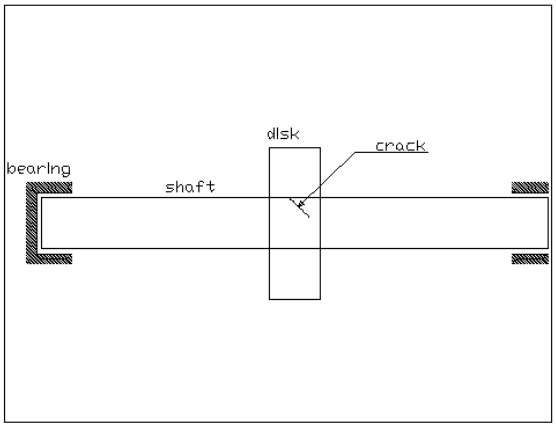

Figure 1: Cracked shaft model

For the crack considered, forces are assumed to be acting in all six directions. The figure 2 below represents the elemental strip of the shaft containing crack and showing all the forces.

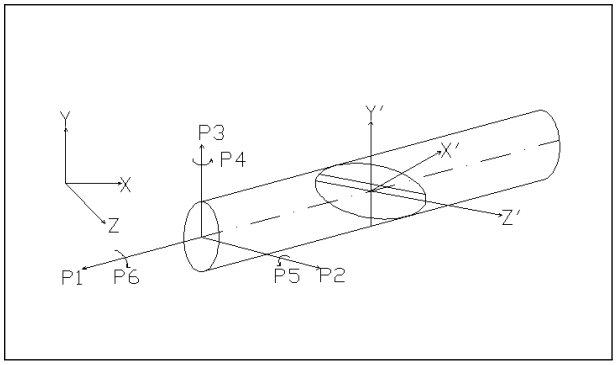

Figure 2: Different forces on the rotor shaft

Where *P1* is axial thrust, *P2* and *P3* are shear forces, *P4* and *P5* are the bending forces resulting in bending moment and *P6* is the force responsible for transmitting torsional moment. So for a shaft of radius $R = D/2$, let us assume a crack of depth a is present in middle of the shaft. Then flexibility of the cracked shaft can be obtained by using stain energy density function and stress intensity factor methods.

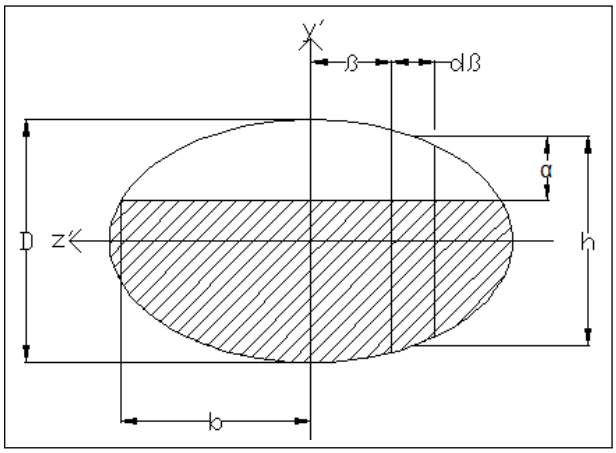

Figure 3: Details of crack

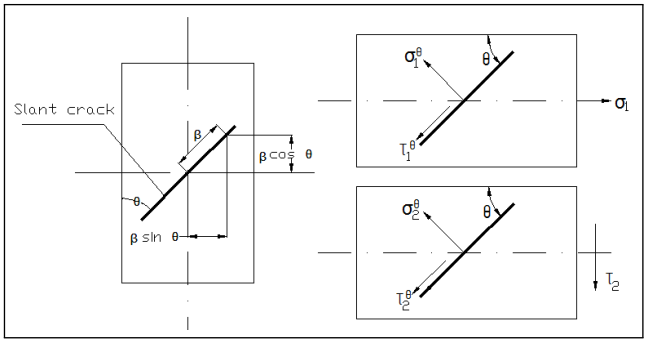

Figure 4: Different components of stresses at crack tip

For the purpose of deriving the flexibility of the shaft the similar approach followed by [8] is used in the analysis. Paris equation gives the additional

displacement u_i of the shaft due to a crack depth a, in the i direction, as

$$U_i = \frac{\partial}{\partial P_i}[\int\int J(a)dA] \quad (1)$$

Where, $J(\alpha)$ is the strain energy density function (SEDF) and P_i is the corresponding load. The SEDF is

$$J(a) = \frac{1}{E'}((\sum_{i=1}^{6} K_I^i)^2) + ((\sum_{i=1}^{6} K_{II}^i)^2) + ((\sum_{i=1}^{6}(1+\nu)K_{III}^i)^2) \quad (2)$$

Where $E' = E/(1-\nu^2)$ for plane strain case considered, E is the modulus of elasticity, ν is the Poisson ratio ($\nu = 0.3$ for steel). K_I^i, K_{II}^i and K_{III}^i are the stress intensity factors (SIF) for the opening, sliding and tearing mode respectively.

The local flexibility due to the crack per unit width is,

$$C_{ij} = \frac{\partial u_i}{\partial P_j} = \frac{\partial^2}{\partial P_i \partial P_j}[\int_0^a J(a)da] \quad (3)$$

For the total width of the crack i.e. $2b$

$$C_{ij} = \frac{\partial^2}{\partial P_i \partial P_j}[\int_{-b}^{b}\int_0^a J(a)dadb] \quad (4)$$

The value of stress intensity factor in equation (2) are well known from the literature [11] for a strip of unit thickness with a transverse crack. But for a slant crack the value of stress intensity factors are unknown but the various researchers have contributed their effort in formulating the stiffness value. In this particular thesis the work of [7] is followed for determination of SIFs.

SIF for mode I (opening mode):

$$K_l^1 = \frac{P_1}{2\pi R^2}\sqrt{\pi\alpha}F_1(\alpha/h) \quad (5)$$

$$K_l^4 = \frac{\sqrt{2}P_4\beta}{\pi R^4}\sqrt{\pi\alpha}F_1(\alpha/h) \quad (6)$$

$$K_l^5 = \frac{\sqrt{2}P_s}{\pi R^4}\sqrt{2R^2-\beta^2}\sqrt{\pi\alpha}F_2(\alpha/h) \quad (7)$$

There will be some extra SIFs in case of slant crack when compared to the transverse crack these extra component of SIF comes due to the orientation of crack with respect to the shaft axis. Because of the orientation, the torsional moment and bending moment also leads to opening mode. Similarly, axial load component also leads to the sliding and tearing mode [7]. So, the normal stress components generated by shearing stress which leads to the opening mode are given as;

$$K_l^6 = \frac{P_6}{\pi R^4}\sqrt{2R^2-\beta^2}\sqrt{\pi\alpha}F_2(\alpha/h) \quad (8)$$

$$K_l^2 = \frac{kP_2}{\pi R^2}\sqrt{\pi\alpha}F_1(\alpha/h) \quad (9)$$

$$K_l^3 = 0 \quad (10)$$

Stress intensity factors for mode II (sliding mode):

$$K_{II}^3 = \frac{kP_3}{\sqrt{2}\pi R^2}\sqrt{\pi\alpha}F_{II}(\alpha/h) \quad (11)$$

$$K_{II}^6 = \frac{P_6\beta}{\pi R^4}\sqrt{\pi\alpha}F_{II}(\alpha/h) \quad (12)$$

$$K_{II}^1, K_{II}^2, K_{II}^4, K_{II}^5 = 0 \quad (13)$$

Stress intensity factors for mode III (tearing mode):

$$K_{III}^1 = \frac{P_1}{2\pi R^2}\sqrt{\pi\alpha}F_{III}(\alpha/h) \quad (14)$$

$$K_{III}^4 = \frac{\sqrt{2}P_4\beta}{\pi R^4}\sqrt{\pi\alpha}F_{III}(\alpha/h) \quad (15)$$

$$K_{III}^5 = \frac{\sqrt{2}P_5\sqrt{2R^2-\beta^2}}{\pi R^4}\sqrt{\pi\alpha}F_{III}(\alpha/h) \quad (16)$$

$$K_{III}^2, K_{III}^3, K_{III}^6 = 0 \quad (17)$$

Where, $F_1(\alpha/h) = \sqrt{\frac{\tan\lambda}{\lambda}}[0.752 + 2.02(\alpha/h) + 0.37(1-\sin\lambda)^3]/\cos\lambda$

$F_2(\alpha/h) = \sqrt{\frac{\tan\lambda}{\lambda}}[0.923 + 0.199(1-\sin\lambda)^4]/\cos\lambda$

$F_{II}(\alpha/h) = \frac{1.122-0.561(\alpha/h)+0.085(\alpha/h)^2+0.18(\alpha/h)^3}{\sqrt{1-(\alpha/h)}}$

$F_{III}(\alpha/h) = \sqrt{\frac{\tan\lambda}{\lambda}}$ And $\lambda = \pi\alpha/(2h)$ Also $k = 6(1+\nu)/(7+6\nu)$ is a shape coefficient for circular cross section. After the substitution of all of the stress intensity factors in Paris equation the flexibility coefficients are obtained and these coefficients are non – dimensionalize by suitable assumption. So the non – dimensionalized flexibility coefficients are as follows;

$$C_{11} = \frac{1}{\pi E' R}[\int_{-\bar{b}}^{\bar{b}}\int_0^{\bar{a}} \frac{\bar{\alpha}}{\sqrt{2}}(F_1^2 + (1+\nu)F_{III}^2)d\bar{\alpha}d\bar{\beta}] \quad (18)$$

$$C_{12} = \frac{1}{\pi E' R}[\int_{-\bar{b}}^{\bar{b}}\int_0^{\bar{a}} \sqrt{2}\bar{\alpha}kF_I^2 d\bar{\alpha}d\bar{\beta}] \quad (19)$$

$$C_{13} = 0 \quad (20)$$

$$C_{14} = \frac{1}{\pi E' R^2}[\int_{-\bar{b}}^{\bar{b}}\int_0^{\bar{a}} 2\sqrt{2}\bar{\alpha}\bar{\beta}(F_1^2 + (1+\nu)F_{III}^2)d\bar{\alpha}d\bar{\beta}] \quad (21)$$

$$C_{15} = \frac{1}{\pi E' R^2}[\int_{-\bar{b}}^{\bar{b}}\int_0^{\bar{a}} 2\sqrt{2}\bar{\alpha}\sqrt{1-\bar{\beta}^2}(F_1F_2 + (1+\nu)F_{III}^2) d\bar{\alpha}d\bar{\beta}]$$

(22)

$$C_{16} = \frac{1}{\pi E' R^2}\left[\int_{-\bar{b}}^{\bar{b}}\int_{0}^{\bar{a}} \sqrt{2}\bar{\alpha}\sqrt{1-\bar{\beta}^2}(F_1F_2)d\bar{\alpha}d\bar{\beta}\right] \quad (23)$$

$$C_{22} = \frac{1}{\pi E' R}\left[\int_{-\bar{b}}^{\bar{b}}\int_{0}^{\bar{a}} 2\sqrt{2}\bar{\alpha}k^2F_1^2d\bar{\alpha}d\bar{\beta}\right] \quad (24)$$

$$C_{23} = 0 \quad (25)$$

$$C_{24} = \frac{1}{\pi E' R^2}\left[\int_{-\bar{b}}^{\bar{b}}\int_{0}^{\bar{a}} 4\sqrt{2}k\bar{\alpha}\bar{\beta}F_1^2d\bar{\alpha}d\bar{\beta}\right] \quad (26)$$

$$C_{25} = \frac{1}{\pi E' R^2}\left[\int_{-\bar{b}}^{\bar{b}}\int_{0}^{\bar{a}} 4\sqrt{2}k\bar{\alpha}\sqrt{1-\bar{\beta}^2}F_1F_2d\bar{\alpha}d\bar{\beta}\right] \quad (27)$$

$$C_{26} = \frac{1}{\pi E' R^2}\left[\int_{-\bar{b}}^{\bar{b}}\int_{0}^{\bar{a}} 4\sqrt{2}k\bar{\alpha}\sqrt{1-\bar{\beta}^2}F_1F_2d\bar{\alpha}d\bar{\beta}\right] \quad (28)$$

$$C_{33} = \frac{1}{\pi E' R}\left[\int_{-\bar{b}}^{\bar{b}}\int_{0}^{\bar{a}} \sqrt{2}\bar{\alpha}k^2F_{II}^2d\bar{\alpha}d\bar{\beta}\right] \quad (29)$$

$$C_{34} = 0 \quad (30)$$

$$C_{35} = 0 \quad (31)$$

$$C_{36} = \frac{1}{\pi E' R^2}\left[\int_{-\bar{b}}^{\bar{b}}\int_{0}^{\bar{a}} 2\sqrt{2}\bar{\alpha}\bar{\beta}kF_{II}^2d\bar{\alpha}d\bar{\beta}\right] \quad (32)$$

$$C_{44} = \frac{1}{\pi E' R^3}\left[\int_{-\bar{b}}^{\bar{b}}\int_{0}^{\bar{a}} 8\sqrt{2}\bar{\alpha}\bar{\beta}^2(F_1^2+(1+\nu)F_{III}^2)d\bar{\alpha}d\bar{\beta}\right] \quad (33)$$

$$C_{45} = \frac{1}{\pi E' R^3}\left[\int_{-\bar{b}}^{\bar{b}}\int_{0}^{\bar{a}} 8\sqrt{2}\bar{\alpha}\bar{\beta}\sqrt{1-\bar{\beta}^2}(F_1F_2+(1+\nu)F_{III}^2)d\bar{\alpha}d\bar{\beta}\right] \quad (34)$$

$$C_{46} = \frac{1}{\pi E' R^3}\left[\int_{-\bar{b}}^{\bar{b}}\int_{0}^{\bar{a}} 8\sqrt{2}\bar{\alpha}\bar{\beta}\sqrt{1-\bar{\beta}^2}F_1F_2d\bar{\alpha}d\bar{\beta}\right] \quad (35)$$

$$C_{55} = \frac{1}{\pi E' R^3}\left[\int_{-\bar{b}}^{\bar{b}}\int_{0}^{\bar{a}} 8\sqrt{2}\bar{\alpha}(1-\bar{\beta}^2)[F_2^2+(1+\nu)F_{III}^2]d\bar{\alpha}d\bar{\beta}\right] \quad (36)$$

$$C_{56} = \frac{1}{\pi E' R^3}\left[\int_{-\bar{b}}^{\bar{b}}\int_{0}^{\bar{a}} 8\sqrt{2}\bar{\alpha}(1-\bar{\beta}^2)F_2^2d\bar{\alpha}d\bar{\beta}\right] \quad (37)$$

$$C_{56} = \frac{1}{\pi E' R^3}\left[\int_{-\bar{b}}^{\bar{b}}\int_{0}^{\bar{a}} 2\sqrt{2}\bar{\alpha}[(1-2\bar{\beta}^2)F_2^2+2\bar{\beta}^2F_{II}^2]d\bar{\alpha}d\bar{\beta}\right] \quad (38)$$

Based on strength of material the flexibility coefficient of the healthy crack can be calculated as

$$C_{ij}^H = \begin{bmatrix} \frac{L}{AE} & 0 & 0 & 0 & 0 & 0 \\ 0 & \frac{L^3}{48EI} & 0 & 0 & 0 & 0 \\ 0 & 0 & \frac{L^3}{48EI} & 0 & 0 & 0 \\ 0 & 0 & 0 & \frac{L}{12EI} & 0 & 0 \\ 0 & 0 & 0 & 0 & \frac{L}{12EI} & 0 \\ 0 & 0 & 0 & 0 & 0 & \frac{L}{2GJ} \end{bmatrix}$$

Where $A = \pi R^2$ is the area of the shaft section, $I = (\pi R^4)/4$ is the area moment of inertia, $J = (\pi R^4)/2$ is the polar moment of inertia and $G = E/2(1+\nu)$is the shear modulus. Similarly the additional flexibility due to the slant crack oriented at 45^0 is given by

$$C_{ij}^C = \begin{bmatrix} C_{11} & C_{12} & 0 & C_{14} & C_{15} & C_{16} \\ C_{21} & C_{22} & 0 & C_{24} & C_{25} & C_{26} \\ 0 & 0 & C_{33} & 0 & 0 & C_{36} \\ C_{41} & C_{42} & 0 & C_{44} & C_{45} & C_{46} \\ C_{51} & C_{52} & 0 & C_{54} & C_{55} & C_{56} \\ C_{61} & C_{62} & C_{63} & C_{64} & C_{65} & C_{66} \end{bmatrix}$$

So the total flexibility coefficient is obtained as

$$C = C_{ij}^{Healthy} + C_{ij}^{Cracked} \quad (39)$$

So by taking the inverse of the flexibility matrix we can obtain he stiffness matrix as

$$K = C^{-1} \quad (40)$$

From above two matrices we can observe that the flexibility in case of cracked rotor is more populated than that of the healthy shaft. This is due to the orientation of the crack which leads to the coupling of different forces in contributing the stress intensity factors.

3. Equation of Motion

The equation of motion of the rotor shaft is derived by assuming single disc Jeffcott rotor mounted on rigid bearings as shown in figure 5. The shaft is considered elastic and massless and the disc is mounted at mid span thus gyroscopic effects are neglected. To derive the equation of motion three degrees of freedom are used and the equation of motion is expressed in terms of rotating co - ordinate. x,y and z are stationary co-ordinate and u,ξ and η are the rotating co-ordinate which revolves with angular speed ω which is same as the rotation of shaft about its own axis. Where ξ,η represent the transverse translation and u represents the axial translation. Following transformation matrix is used to transform the equation of motion from stationary co – ordinate to the rotating one.

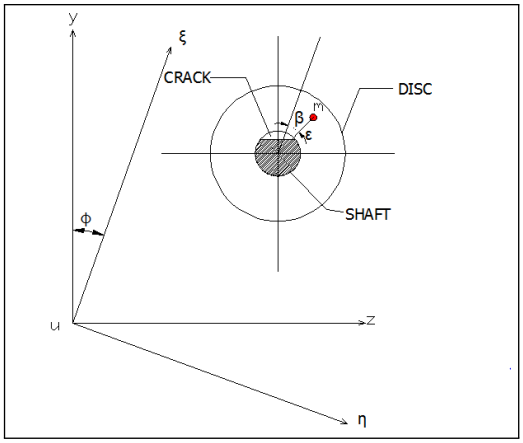

Figure 5: Shaft cross section showing crack

$$\begin{bmatrix} x \\ y \\ z \end{bmatrix} = \begin{bmatrix} 1 & 0 & 0 \\ 0 & \cos\phi & \sin\phi \\ 0 & -\sin\phi & \cos\phi \end{bmatrix} \begin{bmatrix} u \\ \xi \\ \eta \end{bmatrix} \tag{41}$$

So the equation of motion in terms of the rotating co – ordinate can be written as;

$$m[\ddot{\xi} - 2\omega\dot{\eta} - \omega^2\xi] + c[\dot{\xi} - \omega\eta] + k_{51}u + k_{54}\eta + k_{55}\xi = m\varepsilon\omega^2\cos\psi - mg\cos\phi \tag{42}$$

$$m[\ddot{\eta} + 2\omega\dot{\xi} - \omega^2\eta] + c[\dot{\eta} + \omega\xi] + k_{41}u + k_{44}\eta + k_{45}\xi = m\varepsilon\omega^2\sin\psi + mg\sin\phi \tag{43}$$

$$m\ddot{u} + c\dot{u} + k_{11}u + k_{14}\eta + k_{15}\xi = 0 \tag{44}$$

Form the equation of motion we can see that the stiffness coefficients are coupled and the term on the right hand side of the equation indicate the vibration of the shaft is forced vibration due to the presence of unbalance and gravity whereas the last equation is free vibration. Since these equations are coupled so they must be solved simultaneously to get the response.

4. Results and Discussion

4.1 Variation of Stiffness with Crack Depth Ratio

To show the analytical formulation in real case scenarios the rotor shaft detail data is taken from [8]. The detail dimension of shaft with crack is assumed as; radius $R = 0.01m$, length $L = 1m$, modulus of elasticity $E = 2.1 \times 10^{11} N/m^2$, and poisons ratio $\nu = 0.3$, so the stiffness matrices for the shaft without a crack and for the shaft with a crack depth $\alpha/R = 0.3$ are respectively, in N/m,

$$[K^H] = \begin{bmatrix} 65973446 & 0 & 0 & 0 & 0 & 0 \\ 0 & 79168 & 0 & 0 & 0 & 0 \\ 0 & 0 & 79168 & 0 & 0 & 0 \\ 0 & 0 & 0 & 19792 & 0 & 0 \\ 0 & 0 & 0 & 0 & 19792 & 0 \\ 0 & 0 & 0 & 0 & 0 & 2537 \end{bmatrix}$$

$$[K^c] = \begin{bmatrix} 72333681 & -352 & 0 & 0 & -20312 & -1518 \\ -352 & 86997 & 0 & 0 & -25 & -3 \\ 0 & 0 & 86998 & 0 & 0 & 0 \\ 0 & 0 & 0 & 21190 & 0 & 0 \\ -20312 & -25 & 0 & 0 & 19924 & -199 \\ -1518 & -3 & 0 & 0 & -199 & 2783 \end{bmatrix}$$

From these stiffness matrices we can observe that due to the presence of crack in the shaft stiffness coefficients values are reduced and rate of reduction is more in axial and bending directions respectively. The variation of stiffness with crack depth ratio (α/R) is plotted and shown in figure below;

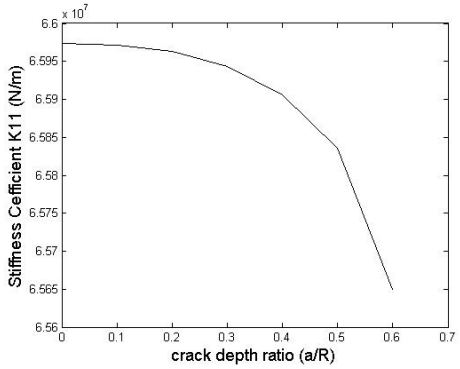

Figure 6: Variation of K11 with crack depth ratio

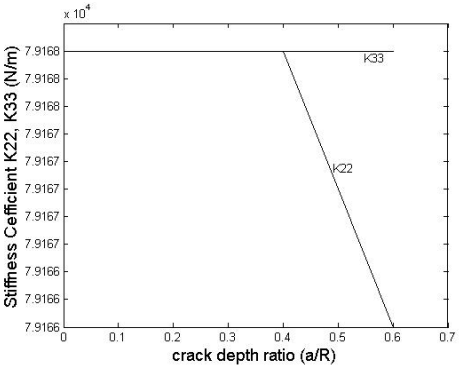

Figure 7: Variation of K22 and K33 with crack depth ratio

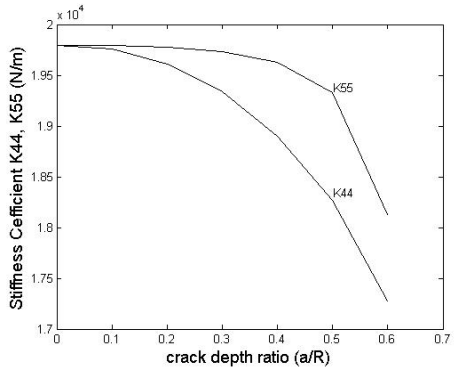

Figure 8: Variation of K44 and K55 with crack depth ratio

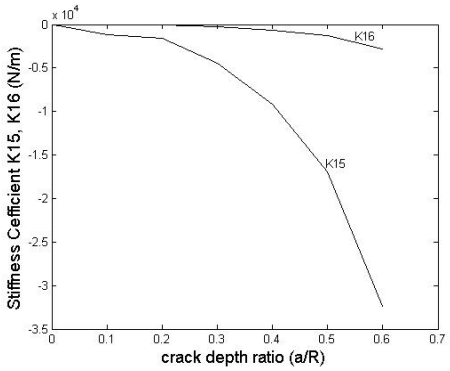

Figure 11: Variation of K15 and K16 with crack depth ratio

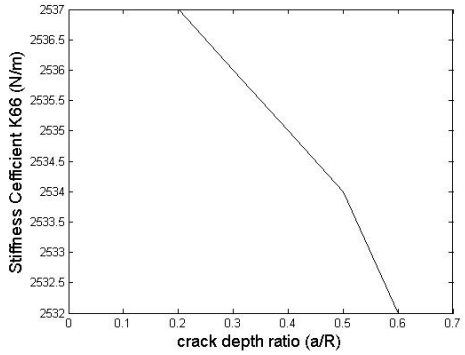

Figure 9: Variation of K66 with crack depth ratio

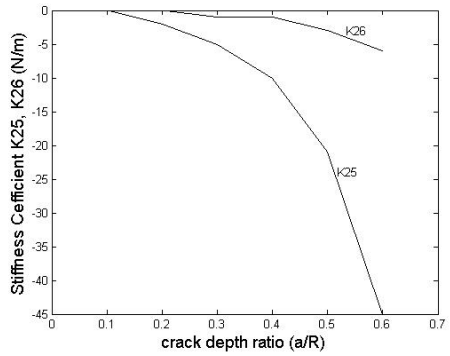

Figure 12: Variation of K25 and K26 with crack depth ratio

As we can see from the above graphs all the values of the stiffness coefficients are deceasing except *K33* as the values of crack depth ratio increases from 0 to 0.6. This is due to the reduction in moment of inertia of the cross section. So the bigger the size of crack in the shaft lesser is the stiffness of the shaft. The value of stiffness coefficient *K33* is not affected by increasing crack depth ratio and the magnitude of other stiffness coefficients *K13*, *K14*, *K23*, *K24*, *K34*, *K35*, *K36*, *K45*, *K46* and their symmetric terms are zero.

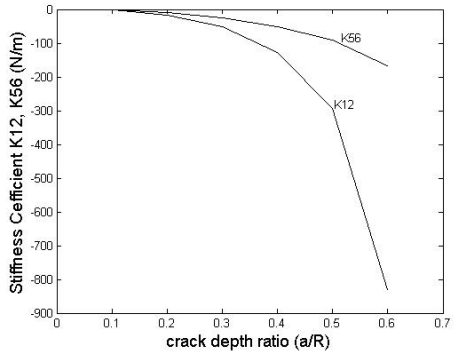

Figure 10: Variation of K12 and K56 with crack depth ratio

4.2 Dynamic response of shaft

To get the dynamic response, first of all the equation of motion are non - dimensionalized and the equations of motions are reduced in to the first order system of differential equations. The equation of motion are solved using fourth order Runge - Kutta method, and the response of healthy shaft as well as the cracked shaft having crack depth ratio o.5 are plotted in time domain as shown in figures below:

4.2.1 Response for axial vibration

The response of healthy as well as the cracked shaft in axial direction is plotted and shown in the figure 13 and figure 14 below.

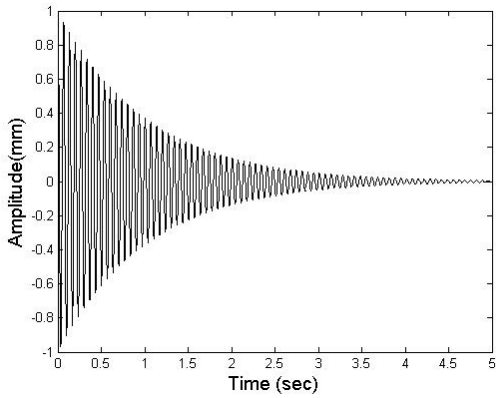

Figure 13: Response of healthy shaft

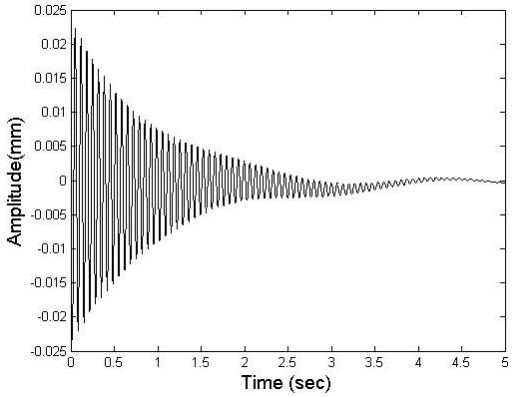

Figure 14: Response of cracked shaft

Comparing the above graphs we can see that the amplitude of the healthy shaft is in the range of 1 mm whereas the amplitude of the cracked shaft is in the range of 0.035 mm. The signal in case of the healthy shaft oscillates about the zero amplitude until the signal dies out but in case of crack rotor the mean position is shifted little bit above the zero amplitude

4.2.2 Response for Z direction vibration

The response of healthy as well as the cracked shaft in bending direction 5 is plotted and shown in figure 15 and figure 16 below.

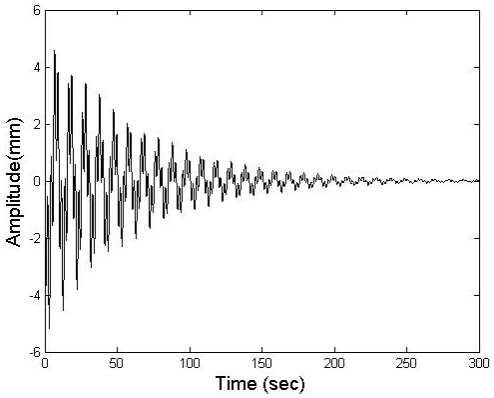

Figure 15: Response of healthy shaft

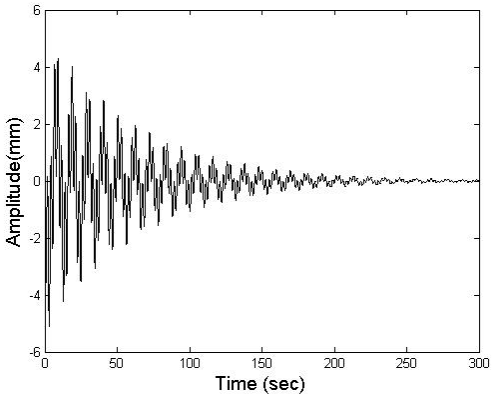

Figure 16: Response of cracked shaft

Comparing the above graphs for the response of healthy rotor and cracked rotor having crack depth ration 0.5 for 300 seconds, we can see that the amplitude of the healthy shaft is more than 4.5 mm whereas the amplitude of the cracked shaft is less than 4.5 mm. So, decrease in amplitude is observed in this case also.

4.2.3 Response for Y direction vibration

The response of healthy as well as the cracked shaft in bending direction 4 is plotted and shown in the figure 17 and figure 18 below.

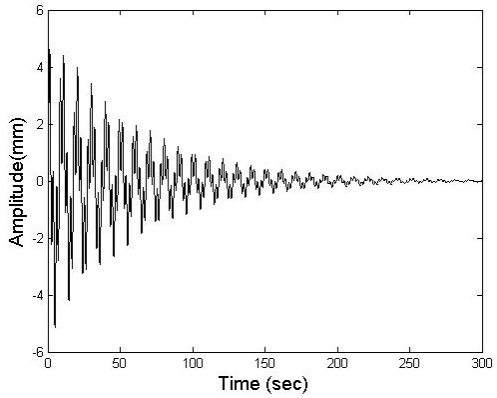

Figure 17: Response of healthy shaft

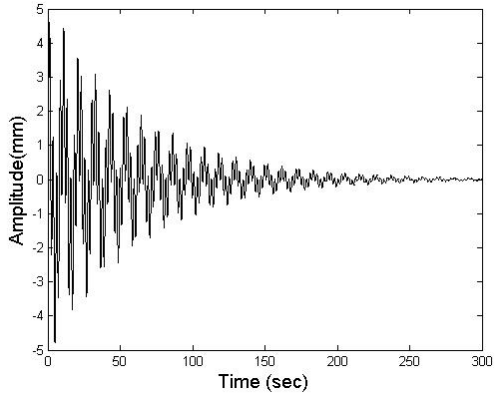

Figure 18: Response of the cracked shaft

From above figure we can observe that the peak amplitude of healthy shaft is around 5 mm and the amplitude of the cracked shaft is around 4.8 mm. Also we can see the rate of decrease in amplitude of the cracked is more compared to the rate of decrease in amplitude of the healthy shaft.

Form the above figures we can say that in general the presence of crack result in decrease in amplitude of the vibration in all directions but the rate of decrease is more in axial direction. The presence of crack means that there is void in a continuous material that means air will fill that void so, that air act as a damping material in a shaft and hence the decrease in amplitude results.

For the calculation of the natural frequency of healthy as well as the cracked shaft the eigen value analysis was carried out and the obtained results are listed in Table 1. From the table, it is observed that the presence of crack in the shaft results in decrease in natural frequency in all directions. This is because the presence of crack in the shaft reduce the stiffness of the shaft and hence the natural frequency. But we can observe the considerable amount of reduction in natural frequency is in torsional direction followed by shear 2 direction, shear 3 direction, axial direction and bending directions respectively.

Table 1: Comparison of natural frequency of healthy and cracked shaft

Directions	Healthy shaft (rad/s)	Cracked shaft (rad/s)
Axial	30.479	29.0516
Shear 2	85.1469	78.0256
Shear 3	85.1469	80.262
Bending 4	170.29	162.440
Bending 5	170.29	162.4469
Torsion	4915.90	4684.5711

5. Conclusion

The dynamic response of cracked as well as the healthy shaft is studied. The presence of crack in a shaft introduces local flexibility; the amount of additional flexibility due to the crack is formulated using linear elastic fracture mechanics. The variation of stiffness with crack depth ratio is studied and it is found that with increasing the crack depth ratio the stiffness values decreases due to this reason the natural frequency of the cracked shaft also decreased and the amount of reduction is more in torsion and shear direction. The response of cracked as well as the healthy shaft is plotted in time domain and from the dynamic response it is observed that the amplitude of the vibration in all three direction (i.e. axial, and two bending directions) are decreased, the amount of reduction is more in axial direction. Hence we can conclude that the presence of crack in shaft results in decrease in stiffness, natural frequency and amplitude of the vibration and this result can be used to detect the presence of crack in a shaft.

6. Recommendations

Further work is needed to see the effect of varying crack angle and location in the response of the shaft. Response can be studied in frequency domain to reveal other unique characteristics.

7. Acknowledgments

The authors would like to acknowledge Associate Professor Dr. Mahesh Chandra Luintel for his valuable suggestions.

References

[1] Giridhar Sabnavis, R Gordon Kirk, Mary Kasarda, and Dane Quinn. Cracked shaft detection and diagnostics: A literature review. *Shock and Vibration Digest*, 36(4), 2004.

[2] M. Ichimonji and S. Watanabe. The dynamics of a rotor system with a shaft having a slant crack (a qualitative analysis using a simple rotor model). *Japan Society of mechanical engineers*, 31:712–718, 1988.

[3] Andrew D Dimarogonas. Vibration of cracked structures: A state of the art review. *Engineering Fracture Mechanics*, 55(5):831–857, 1996.

[4] A.P. Bovsunovsky. Efficiency analysis of vibration based crack diagnostics in rotating shafts. *Engineering Fracture Mechanics*, 173:118–129, 2017.

[5] Daniel Adofo Ameyaw. Crack detection in shaft using vibration measurements and analysis. Technical report, Kwame Nkrumah University of Science and Technology, 2014.

[6] A. S. Sekhar and B. S. Prabhu. Crack detection and vibration characterstics of cracked shafts. *Journal of Sound and Vibration*, 157:375–381, 1992.

[7] Ashish K Darpe. Dynamics of a Jeffcott rotor with slant crack. *Journal of Sound and Vibration*, 303:1–28, 2007.

[8] C. A. Papadopoulos and A. D. Dimarogonas. Coupled longitudinal and bending vibrations of a rotating shaft with an open crack. *Journal of Sound and Vibration*, 117(1):81–93, 1987.

[9] Ashish K Darpe. Coupled vibrations of a rotor with slant crack. *Journal of Sound and Vibration*, 305(1-2):172–193, 2007.

[10] Fulei Chu Yanli Lin. The dynamic behavior of a rotor system with a slant crack on the shaft. *Mechanical Systems and Signal Processing*, 24:522–545, 2010.

[11] Hiroshi Tada, Paul C. Paris, and George R. Irwin. *Stress Analysis of Cracks Handbook, Third Edition*. ASME press, 2000.